

## Drug Microencapsulation by PLA/PLGA Coacervation in the Light of Thermodynamics. 2. Parameters Determining Microsphere Formation

CLAUDIO THOMASIN, HANS P. MERKLE, AND BRUNO GANDER\*

Contribution from the Department of Pharmacy, ETH, Winterthurerstr. 190, 8057 Zuerich, Switzerland.

Received February 4, 1997. Accepted for publication December 19, 1997.

**Abstract** □ Phase separation (frequently called coacervation) of poly(lactide) (PLA) and poly(lactide-co-glycolide) (PLGA) is a classical method for drug microencapsulation. Here, attempts have been made to describe this process in the light of thermodynamics. Different PLA/PLGAs were dissolved in either dichloromethane or ethyl acetate, phase separated by addition of the coacervating agent silicone oil (PDMS), and hardened in either octamethylcyclotetrasiloxane or hexane. Various stages of phase separation were defined microscopically, and the coacervate and continuous phases characterized with respect to volume, composition, polymer molecular weight, and rheological behavior. The optimal amount of PDMS was inversely proportional to the polymer molecular weight and hydrophilicity, and a coacervate viscosity of above 5–10 Pa s was required for stable coacervate droplets. The composition and, consequently, viscosity of the coacervate and continuous phases depended on the polymer-solvent-PDMS interactions, as analyzed by the parameters  $\chi$  (Flory),  $\delta$  (Hildebrand), and  $\Delta_{\text{int}}E$  (Hö). In general, the lattice model of Flory and Scott describing polymer-polymer incompatibility best explained the results. The interaction parameters and viscosity of the phases were also helpful to explain microsphere characteristics such as residual solvent and particle size. The data suggest that microsphere formation by polyester coacervation is primarily driven by molecular interactions between polymer, solvents, and coacervating agent.

### Introduction

Biodegradable microspheres of poly(lactide) (PLA) or poly(lactide-co-glycolide) (PLGA) have received considerable attention as delivery systems for peptide and protein drugs. Microencapsulation methods have been developed respecting the particular properties of this category of compounds. Although most of the more recent microencapsulation studies focused on the process of solvent evaporation or extraction,<sup>1</sup> phase separation remains very attractive for highly water soluble compounds. Incidentally, the terms “phase separation” and “coacervation” will be used interchangeably in this text, because the latter is a very commonly used term to describe PLA/PLGA microsphere formation by phase separation. Initial work on peptide microencapsulation in PLA/PLGA by phase separation was performed in the early 1980s.<sup>2–5</sup> However, these studies did not especially explore the crucial properties of solvents, coacervating agents, and polymers. More insight into the phase separation process was gained when the different consecutive steps of PLGA phase separation in a dichloromethane/silicone oil system were described.<sup>6,7</sup> These different steps were shown to be influenced by the molec-

ular weight distribution, conformation and hydrophobicity of the polymer and by the amount and viscosity of the coacervating agent. Recently, the importance of basic physicochemical parameters of PLGA coacervation and coacervation kinetics for the formation of empty and drug-loaded microspheres was demonstrated.<sup>8</sup> Besides, only little information is available on the mechanisms of PLA/PLGA phase separation under conditions relevant for drug microencapsulation, although fundamental aspects of polymer phase separation have been covered thoroughly some time ago (reviewed in part 1).<sup>9</sup> Nonetheless, Hildebrand and Hansen solubility parameters have been considered in the phase separation of ethylcellulose to form microcapsules.<sup>10–12</sup> Further, a new thermodynamic model has also been developed to quantify drug-polymer-solvent interactions and to characterize and predict aqueous protein encapsulation into PLA/PLGA microspheres by spray-drying.<sup>13</sup>

In this study, the process of phase separation of various types of PLA/PLGA was analyzed in some detail by establishing phase diagrams defining the various stages of phase separation and by characterizing the coacervate and continuous phases in terms of volume, composition, polymer molecular weight, and rheological behavior. Attempts were made to interpret the results in thermodynamic terms using three different thermodynamic models based on  $\chi$  (Flory),  $\delta$  (Hildebrand) and  $\Delta_{\text{int}}E$  (Hö, 1994). The thermodynamic models used have been described in more detail elsewhere (part 1).<sup>9</sup> Further, the importance of phase separation conditions for the quality of biodegradable polyester microspheres was outlined. Most importantly, the purpose of this study was to examine PLA/PLGA phase separation under conditions relevant for drug microencapsulation and to interpret the observations with the aid of thermodynamic parameters. Clearly, the study was not intended to analyze thermodynamically the PLA/PLGA phase separation.

### Experimental Section

**Materials**—Medical grade poly(D,L-lactide) (PLA) (Resomer-R104, -202, -203, -206, and -209), poly(D,L-lactide-co-glycolide) 75:25 (PLGA 75:25) (Resomer-RG752, -755, and -756), poly(D,L-lactide-co-glycolide) 50:50 (PLGA 50:50) (Resomer-RG502, -503, -504, and -505), and poly(L-lactide) (PLLA) (Resomer-L206) were purchased from Boehringer Ingelheim, Ingelheim, FRG, and used as received. The molecular weights  $\bar{M}_w/\bar{M}_n$  (kDa) of the polyesters, as determined by GPC,<sup>14</sup> were 14.6/7.7 (R202), 23.3/10.6 (R203), 129.7/60.3 (R206), 513.0/232.0 (R209), 17.0/10.5 (RG752), 68.6/38.3 (RG755), 88.2/36.3 (RG756), 13.7/7.4 (RG502), 35.0/15.7 (RG503), 41.2/19.1 (RG504), 68.2/24.4 (RG505), and 69.5/26.9 (L206). For the R104, a  $\bar{M}_w$  of approximately 1.9 kDa was indicated by the manufacturer. As certified by the manufacturer, residual monomer content was below 0.5% and residual acetone was below 0.1%

\* Tel: +41 1 635 60 12. Fax: +41 1 635 68 81. E-mail: bruno.gander@pharma.ethz.ch.

for all samples. Dichloromethane (DCM) and ethyl acetate (EtAc) (analytical grade, >99.5%) were from Merck, Darmstadt, FRG. Hexane (Hex) and silicone oil DC-200 (PDMS) of different viscosity (110, 375, 1070 mPa s) were obtained from Fluka, Buchs, Switzerland. Octamethylcyclotetrasiloxane (OMCTS) was from Scheller, Zürich, Switzerland. PDMS of 3000 mPa s was prepared by mixing aliquots of PDMS of 1070 and 10 700 mPa s (Plüss & Stauffer, Oftringen, Switzerland) according to a viscosity-nomogram.<sup>15</sup> DCM and EtAc served as polymer solvents, PDMS as coacervating agent, Hex and OMCTS as hardening agents to solidify the microspheres.

**Solubility Parameters**—The Hansen parameters of PLA were determined theoretically according to a group contribution method.<sup>16</sup> The theoretical values were compared to those estimated experimentally through the solubility behavior of PLA in three solvent classes differing in their hydrogen-bonding capability.<sup>17</sup> Typically, 200 mg of polymer was mixed with 4 mL of solvent, and the mixture was shaken vigorously and examined for complete solubility at  $20 \pm 1$  °C. All solvents that did not completely dissolve the polymer were also tested at 50 °C. Solvents inducing only polymer swelling or causing turbidity were classified as nonsolvents. For the copolymers PLGA 75:25 and 50:50, the solubility parameter  $\delta$  was estimated experimentally rather than calculated from group contributions.

**Phase Diagrams of PLA/PLGA Coacervation**—A 20 g portion of 2.5, 5.0, or 10.0% (w/w) polymer solutions in DCM, using different PLAs and PLGAs 75:25 and 50:50, was mechanically stirred at 250 rpm in an airtight two-neck round-bottom flask kept at  $15 \pm 1$  °C. Methylene blue (Fluka, CH-Buchs) was dissolved in the organic solution to enhance optical contrasts in the coacervation mixtures. Aliquots of PDMS were added at 2 min intervals to increase the amount of nonsolvent by 2–5% relative to the total weight. Before each new silicone oil addition, 0.2 mL of the mixture were withdrawn, examined, and photographed under an optical microscope (Optiphot with Microflex UFX, Nikon, JPN-Tokyo). From the appearance, size, and stability of the droplets, phase diagrams were established. For PLA R202, the experiment was done in both DCM (Lewis acid) and EtAc (Lewis base) to study the influence of the solvent type. Silicone oil addition and withdrawal of coacervation mixture was done through an inserted Teflon tube under rigorous precautions to prevent loss of the highly volatile solvents.

**GPC of Coacervated Polymers**—For two different DCM/PDMS ratios, the coacervate phases were separated by centrifugation and collected with a syringe. DCM was evaporated to avoid interference in the GPC chromatogram, and the polymer was redissolved in tetrahydrofuran (THF) spiked with toluene. GPC conditions were identical with those described elsewhere.<sup>14</sup>

**Appearance, Volume, and Composition of Coacervate and Continuous Phases**—The influence of polymer type and molecular weight on the appearance and the volume of the coacervate phase was determined at  $15 \pm 1$  °C for three different solvent/nonsolvent ratios. For this, concentrations of 2.5, 5.0, and 10% (w/w) of poly(L-lactide) and poly(D,L-lactide) were dissolved in DCM and supplemented by varying amounts of PDMS. The dispersions were transferred into graduated vials and centrifuged at  $3500 \text{ min}^{-1}$  for 15 min. The separated coacervate and continuous phases were examined for their appearance and volume fractions. The experiments were conducted in sealed containers to prevent loss of the volatile DCM.

The actual composition of the continuous and coacervate phases was determined for the coacervation mixtures containing 1 g of PLA R202, 19 g of DCM, and increasing amounts (5–46 g) of PDMS. First, the theoretical solvent content of the continuous liquid was calculated from the difference of volumes between the continuous phase and the added PDMS. This calculation was made under the assumptions that all PDMS remains in the continuous phase and no volume change occurs upon mixing DCM and PDMS. The DCM content of the coacervate was calculated from the difference between the total amount of DCM used (19 g) and the estimated amount in the continuous liquid. The calculated results were verified gravimetrically with 5 mL of the continuous phase, after evaporation of DCM at 150 °C.

**Rheological Behavior of Coacervate and Continuous Phases**—The rheological behavior of the coacervate phase, isolated at different solvent/nonsolvent ratios, was determined for poly(L-lactide) and poly(D,L-lactide) at polymer concentrations of 2.5, 5, and 10% (w/w) with a plate and cone sensor viscometer (Rheovisc

12, Haake, Karlsruhe, FRG). For this, the coacervate dispersions were centrifuged at  $3500 \text{ min}^{-1}$  in sealed vials and cooled to 10 °C. Shear stress was recorded in a solvent saturated atmosphere (glass chamber sealed over the sensor; Contraves, Oerlikon, Switzerland) for 1 min by increasing automatically the shear rate from 100 to  $1000 \text{ min}^{-1}$ . The temperature was maintained at  $15 \pm 1$  °C for all experiments.

The viscosity of the continuous liquid was determined in a cylinder-type viscometer (VT 501, Haake, Karlsruhe, FRG) at increasing and decreasing shear rates of 27–2700  $\text{s}^{-1}$ .

**Turbidity of Coacervation Dispersions**—The stability of coacervate droplets against merging and sedimentation was characterized by monitoring light transmission at 600 nm (UV/VIS-200, Perkin-Elmer Überlingen, FRG) of coacervate dispersions prepared at different solvent/nonsolvent ratios.

**Preparation of Microspheres**—Empty and BSA-loaded microspheres were prepared by dissolving the polymer (2 g) in DCM or EtAc at concentrations of 2.5, 5.0, or 10% (w/w). Half of the volume of the respective solutions was transferred into a jacketed-vessel (250 mL) equipped with baffles and an anchor stirrer. The protein solution (500  $\mu\text{L}$ ) was emulsified in the other half of the polymer solution by ultrasonication, and this dispersion was also added to the vessel. Coacervation was induced by introducing a predetermined amount of silicone oil at a rate of  $4 \text{ g min}^{-1}$  to obtain stable coacervate droplets according to established phase diagrams. Unless specified otherwise, stirring was set at  $1000 \text{ min}^{-1}$  and the temperature maintained at 10–15 °C. The coacervation dispersion was slowly transferred into 1200 mL of hardening agent to solidify the microparticles. Stirring was continued for 30 min whereafter the microspheres were collected on a sintered glass filter and washed with 100 mL of hexane. The microparticles were air-dried for 5 min and resuspended three times in water containing 0.1% poloxamer F 68 (ICI, Cleveland, UK). After washing, the powder was dried for 12 h under laminar air flow followed by vacuum-drying at 0.5 mbar.

**Residual Solvents in the Microspheres**—BSA-loaded microspheres prepared at three different DCM/PDMS ratios were analyzed by GC for their solvent and hardening agent content. Typically, 100 mg of each sample were weighed into screw-cap vials and dissolved in 2.0 g of 1,4-dioxane. The dispersions were centrifuged at 3000 rpm for 10 min. The solutions were cooled to 10 °C, and the clear supernatant subsequently transferred into 1 mL HPLC vials and sealed. Analysis was performed on a GC 8500 (Perkin-Elmer, Überlingen, FRG) using a 10 m wide bore fused silica column of 0.53 mm internal diameter, an additional retention gap of 1.0 m, a stationary phase of 5  $\mu\text{m}$  methylsilicone (PS 255) cross-linked with 2% dicumyl peroxide (BGB, Adliswil, Switzerland), and the carrier gas nitrogen with a flow rate equivalent to a retention time for methane of 35 s. The injected volume was 2.0 mL and the injector temperature set at 200 °C. The oven temperature was set at 40 °C for 5 min and then increased to 200 °C at a rate of  $15 \text{ °C min}^{-1}$ . The total analysis time was 40 min. The solvents were detected by high-sensitivity FID at 250 °C.

**Size Distribution of Microspheres**—Microspheres were characterized for their particle size by laser light diffraction (Mastersizer SX, Malvern, Malvern, UK), as described elsewhere.<sup>14</sup> Calculations were based on Mie's theory accounting for the optical properties of the polymer used. The refractive index of PLA and PLGA was determined according to a group contribution method.<sup>16</sup>

## Results

### Solubility Behavior of PLA/PLGA in Different Solvent Classes

The solubility range of PLA and PLGA in solvents with different hydrogen-bonding capacity is presented in Table 1. All three polyester types were completely insoluble in solvents of strong hydrogen-bonding capacity. By contrast, the solubility range in solvents of poor or intermediate hydrogen-bonding depended on the polymer type. Generally, moderate H-bonding solvents showed the widest solubility range, which decreased in the order PLA > PLGA 75:25 > PLGA 50:50. Poor hydrogen-bonding solvents with  $<17.8 \text{ MPa}^{0.5}$  were classified here as nonsolvents.

The thermodynamic parameters of the components used in the coacervation process are compiled in Table 2. The

**Table 1—Solubility Parameter Range of PLA and PLGA Polymers**

H-bonding capacity of solvents	$\delta$ -range			
	of solvents tested <sup>37</sup> (MPa <sup>0.5</sup> )	for PLA (MPa <sup>0.5</sup> )	for PLGA75:25 (MPa <sup>0.5</sup> )	for PLGA50:50 (MPa <sup>0.5</sup> )
poor	14.1–26.0	17.8–26.0	18.8–26.0	19.0–26.0
moderate	15.1–30.1	17.4–30.1	17.4–30.1	18.2–30.1
strong	19.4–29.7	not soluble	not soluble	not soluble

**Table 2—Thermodynamic Parameters for the Components Used in PLA Microencapsulation<sup>16,19,26,37–39</sup>**

component	molec wt (g mol <sup>-1</sup> )	molar volume (cm <sup>3</sup> mol <sup>-1</sup> )	Hansen			Drago		Hildebrand <sup>d</sup> $\delta$ (MPa <sup>0.5</sup> )
			$\delta_d$	$\delta_p$	$\delta_h$	$E$ (kJ <sup>0.5</sup> mol <sup>-0.5</sup> )	$C$	
PLA	72.0 <sup>b</sup>	56.5	15.8 <sup>c</sup>	8.7 <sup>c</sup>	11.1 <sup>c</sup>	3.31 <sup>d</sup>	2.00 <sup>d</sup>	20.8 (m)
DCM	84.9	63.9	18.2	6.3	6.1	1.76	0.23	19.8 (p)
EtAc	88.1	98.5	15.8	5.3	7.2	3.31	2.00	18.6 (m)
PDMS	74.1 <sup>b</sup>	76.0	15.5	1.6	3.5	3.44 <sup>e</sup>	3.07 <sup>e</sup>	15.5 (p)
OMCTS	74.1 <sup>b,f</sup>	76.0 <sup>f</sup>	15.5 <sup>f</sup>	1.6 <sup>f</sup>	3.5 <sup>f</sup>	3.44 <sup>f</sup>	3.07 <sup>f</sup>	13.1 (p)
hexane	84.0	131.6	14.9	0	0	0	0	14.9 (p)

<sup>a</sup> p and m indicate poor and moderate H-bonding solvents. <sup>b</sup> Values for the repeating unit of the polymers. <sup>c</sup> Values calculated from group contributions. <sup>d</sup> True values not available; values adopted from EtAc. <sup>e</sup> True values not available; values adopted from CH<sub>3</sub>OCH<sub>3</sub>. <sup>f</sup> Values adopted from PDMS.

Hansen parameters of PLA were calculated according to a group contribution method;<sup>16</sup> for the copolymers,  $\delta$  cannot be calculated accurately by this method, because of the nonrandom distribution of the repeating units. As expected, the solubility parameters of the coacervating (PDMS) and hardening agents (OMCTS, hexane) are far beyond the solubility range of PLA, whereas the  $\delta$  values of the solvents DCM and EtAc are in the same range as the  $\delta$  of the polymer.

This solubility behavior was also in agreement with the estimated interaction parameters between various pairs of compounds used in the coacervation process. The values in Table 3 were calculated according to three molecular interaction models, as presented in more detail in part 1 of this contribution:<sup>9</sup>

$$\chi \approx \frac{V_1}{RT}(\delta_2 - \delta_1)^2 \quad (1)$$

$$\Delta\delta = [4(\delta_{d1} - \delta_{d2})^2 + (\delta_{p1} - \delta_{p2})^2 + (\delta_{h1} - \delta_{h2})^2]^{0.5} \quad (2)$$

$$\Delta_{int}E = -nV_1\delta_{d1}\delta_{d2} - nV_1\delta_{p1}\delta_{p2} - (E_1E_2 + C_1C_2) \quad (3)$$

Generally, intermediate to strong interactions, as represented by low  $\chi$  (Flory) and  $\Delta\delta$  (Hansen) values or high interaction energies,  $\Delta_{int}E$  (H $\delta$ ), were found between the solvents and PLA, on one side, and between the nonsolvents and solvents, on the other side. Moreover, the interactions of solvent–PDMS and solvent–PLA are of similar order of magnitude. This may indicate that polymer desolvation by PDMS proceeds slowly, which should facilitate the control of coacervation and reduce the risk of polymer precipitation. When analyzing the data by a nonparametric correlation test (Spearman), highly significant correlations,  $r_s$ , were found between the rank order of values  $\Delta\delta$  and  $\Delta_{int}E$  ( $r_s = 0.7253$ ), between  $\chi$  and  $\Delta\delta$  ( $r_s = 0.7321$ ), and between  $\chi$  and  $\Delta_{int}E$  ( $r_s = 0.6882$ ) (with  $r_{tab} = 0.643$  for  $\alpha = 0.01$ ).

So far, coacervation was treated here primarily as a desolvation process, for which interaction parameters predict potential PLA/PLGA desolvation by PDMS irrespective of the solvent used. When considering PLA/PLGA coacervation as a polymer 1–polymer 2 repulsion

**Table 3—Calculated Interaction Forces in Binary Mixtures Used for PLA Coacervation**

binary mixtures solvent–solute	$\chi^a$ (eq 1)	$\Delta\delta$ (eq 2) (MPa) <sup>0.5</sup>	$\Delta_{int}E^b$ (eq 3) (kJ mol <sup>-1</sup> )
DCM–PLA	0.03	7.33	-50.04
EtAc–PLA	0.19	5.17	-73.22
PDMS–PLA	0.86	10.42	-37.20
OMCTS–PLA	1.82	10.42	-37.20
hexane–PLA	1.85	14.22	-15.04
DCM–PDMS	0.48	7.62	-44.10
EtAc–PDMS	0.38	5.27	-67.44
DCM–OMCTS	1.16	7.62	-44.10
EtAc–OMCTS	1.20	5.27	-67.44
DCM–hexane	0.62	10.98	-34.66
EtAc–hexane	0.54	9.12	-46.38
OMCTS–PDMS	0.18	0.00 <sup>c</sup>	-58.17
hexane–PDMS	0.02	4.03	-60.79

<sup>a</sup> Calculated for  $T = 298$  °K. <sup>b</sup>  $\Delta_{int}E$  was calculated using  $V_1$  of the more volatile solvent and the  $E$  and  $C$  parameters only for the mixtures where acid–base interactions can occur, i.e., those containing DCM as solvent. <sup>c</sup> Hansen parameters for OMCTS were adopted from PDMS, hence  $\Delta\delta = 0$ .

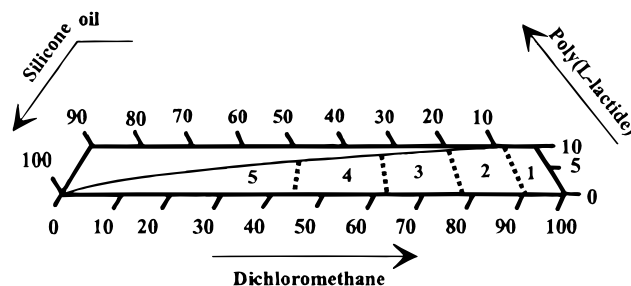


**Figure 1—Phase diagram of poly(L-lactide) characterizing the phase separation process in a DCM/PDMS mixture. The dotted lines represent the boundaries between the stages 1–5, which can be microscopically distinguished during coacervation.**

process, the boundary conditions of PLA phase separation can be calculated, as detailed in part 1.<sup>9</sup> Typically, in a system PDMS/PLA/DCM, with a PDMS of 1070 mPa s ( $\bar{M}_n \approx 26\,500$  and  $x_{2a} \approx 350$ ),<sup>18</sup> and with a PLA of  $\bar{M}_n$  of 7700 ( $x_{2b} \approx 106$ ), a volume fraction  $\phi_1$  of 0.97 DCM was calculated for  $(\chi_c)_{2a,2b}$  according to:

$$(\chi_c)_{2a,2b} = 0.5 \left( \frac{1}{\sqrt{x_{2a}}} + \frac{1}{\sqrt{x_{2b}}} \right)^2 \left( \frac{1}{1 - \phi_1} \right) \quad (4)$$

This equation was explained in more detail in part 1.<sup>9</sup> Therefore, the critical condition for polymer phase separation was reached when the total polymer concentration (PDMS and PLA) was >3%. With the initial PLA concentration of 5–10% used here, phase separation started immediately upon PDMS addition as a result of polymer repulsion.

If, for simplicity, the PLA/PDMS/DCM mixture is considered as an apolar system, phase separation was also supported by the Van Oss theory (part 1).<sup>9</sup> Taking into account the surface tensions of DCM ( $\gamma_1 = 27.2$  mN m<sup>-1</sup>),<sup>20</sup> of PLA ( $\gamma_2 = 40$  mN m<sup>-1</sup>, as estimated from group contributions),<sup>16</sup> and of PDMS ( $\gamma_3 = 21.5$  mN m<sup>-1</sup>),<sup>19</sup> the corresponding equations (eqs 23 and 24 in part 1)<sup>9</sup> predicted polymer phase separation.

**PLA/PLGA Coacervation Phase Diagrams**—The different stages of PLA phase separation are illustrated for PLA L206 in Figure 1. Phase separation of this high molecular weight PLA could be divided into five stages, each of them characterized by a typical microscopic appearance, rheological behavior, and phase volume. Gener-

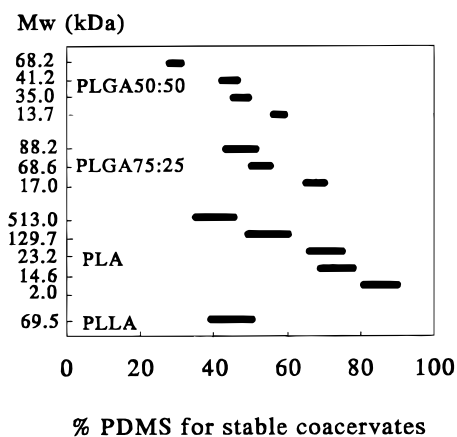


Figure 2—Amounts of PDMS (1070 mPa s) defining the area of stable coacervate droplets for different polymer types and molecular weights.

ally, the following stages were distinguishable: (1) Pseudoemulsion of PDMS droplets in DCM/PLA, (2) mixed phase system of PDMS droplets in DCM/PLA besides DCM/PLA droplets in PDMS, (3) phase inversion and macroscopically detectable phase separation with the DCM/PLA phase starting to form unstable microdroplets merging together, (4) stable dispersion of well-defined coacervate droplets, and (5) aggregation and precipitation of polymer droplets (solid-liquid demixing). The phase borderlines greatly depended on the polymer type and molecular weight and on the interaction between polymer-solvent and solvent-nonsolvent. For microencapsulation, stages 3 and 4 were of utmost importance, as the physicochemical properties of these mixtures were found responsible for the wetting, spreading, and drug engulfment processes.<sup>21</sup>

The stability behavior of the coacervate droplets in stage 4 was critical for the successful transfer of the coacervate dispersion into the hardening agent and the isolation of discrete microparticles therefrom. If the borderline to stage 5 was crossed due to excessive PDMS addition, the coacervate droplets aggregated irreversibly. Uncontrolled phase separation was most critical for PLGA 50:50 and poly(L-lactide), whereas PLGA 75:25 and PLA were more tolerant to aggregation and readily formed single, partly gelled droplets.

The amount of PDMS defining the borderlines of stage 4 and necessary to control the formation of well-defined coacervate droplets was determined for a whole range of polymers (Figure 2). While the homopolymers were characterized by a broad zone of stable coacervates, PLGA 75:25 and even more PLGA 50:50 coacervates were stable only within a narrow range of PDMS concentration. The process of polymer phase separation was fastest for PLGA 50:50, followed by PLGA 75:25 and PLA. Interestingly, the isomeric semicrystalline PLLA was coacervated at a substantially lower PDMS concentration than the racemic amorphous PLA; this reflects another mechanism of phase separation, which is formation of crystalline domains in the phase-separated droplets.<sup>40</sup> Finally, an inverse proportionality was found when the midpoint of the necessary PDMS amount was plotted versus  $\bar{M}_w$  of the polymers; the linear correlation coefficients were  $r = 0.987$  for PLA,  $r = 0.995$  for PLGA 75:25, and  $r = 0.987$  for PLGA 50:50. Although the polymer molecular weight distribution should also affect phase separation, this was not examined in this study, but has been addressed recently by other authors.<sup>6,7</sup>

For PLA, linear correlation applied up to a  $\bar{M}_w$  of 130 kDa. For the 513 kDa PLA (R209), the amount of PDMS (35%) necessary to stabilize the coacervate was higher than expected. In thermodynamic terms, the interactions between polymer and solvent and between solvent and

Table 4—Composition, Volume, and Calculated Solubility Parameter of Coacervate and Continuous Phases of 14.6 kDa PLA upon Addition of Increasing Amounts of PDMS (stages 1–4 of Figure 1) to a Solution of 1 g of PLA in 19 g of DCM<sup>c</sup>

characteristics	coacervation stage							
	1	2	3	4				
composition (% w/w)								
PDMS	20	40	60	70				
DCM	76	57	38	29				
PLA	4	3	2	1				
	Coac <sup>a</sup>	CLiq <sup>b</sup>	Coac <sup>a</sup>	CLiq <sup>b</sup>	Coac <sup>a</sup>	CLiq <sup>b</sup>	Coac <sup>a</sup>	CLiq <sup>b</sup>
volume (mL)	5.4	18.1	3.4	31.6	2.3	40.1	2.0	61.1
DCM content (%)	38.4	61.6	23.7	76.3	15.4	84.6	13.9	86.1
$\delta$ (MPa <sup>0.5</sup> )	19.9	18.2	20.0	17.4	20.1	16.7	20.2	16.4

<sup>a</sup> Coac refers to the coacervate phase. <sup>b</sup> CLiq refers to the continuous liquid. <sup>c</sup> The solvent content of each phase is expressed as percentage of the total amount of solvent used in the coacervation mixtures.

coacervating agent were the most prominent factors controlling coacervation. For illustration, PLA coacervation required a higher percentage of PDMS when the solvent EtAc (76% PDMS) was used instead of DCM (69% PDMS). Obviously, partitioning of EtAc between coacervate and continuous liquid was lower, indicating a relatively weak interaction between this polymer solvent and PDMS.

**Composition of Coacervate and Continuous Liquid**—Table 4 shows some physicochemical characteristics of coacervate and continuous liquids taken from typical stages during coacervation. The polymer selected for this analysis was a low  $\bar{M}_w$  PLA because this polymer type was found less subject to rapid desolvation and solid state aggregation (stage 5). PLA phase separation was induced by very low amounts of PDMS, because a single phase could only be observed at PDMS concentrations <2%. Above this concentration, two distinct phases were detected after centrifugation of the coacervation dispersion. The coacervate phase (Coac) primarily consisted of PLA and DCM, whereas the continuous liquid (CLiq) contained PDMS and DCM. We assume that most of the wall forming polymer had already separated at this stage and that only low  $\bar{M}_w$  lactide oligomers remained possibly in the continuous phase. This assumption was supported by the observation that the evaporation of DCM from the continuous phase did not produce any turbidity. However, the calculated solubility parameter value of CLiq in stage 2 was very close to the solubility range of PLA (17.8–26 MPa<sup>0.5</sup>), indicating that this continuous liquid had enough solvent power for PLA oligomers only. By raising the amount of PDMS from 20 to 70%, the separated PLA phase was continuously desolvated, as reflected by a decrease in the coacervate volume and solvent content. At stage 3, polymer phase separation was complete because the solubility parameter of the continuous liquid was below 17 MPa<sup>0.5</sup> and, hence, outside the  $\delta$ -range of PLA.

With increasing amount of PDMS, DCM was progressively extracted from the coacervate into the continuous phase. At stage 4, approximately 15% of the total DCM content remained in the coacervate phase, which still represented more than 70% of the coacervate mass. Polymer solvation by DCM was still sufficient to prevent uncontrolled gelling or aggregation.

**Molecular Weight of Coacervated Polymers**—The chromatographic analysis of PLA and PLGA coacervates did not reveal any fractionation of polymer molecular weight at the end of PDMS addition, irrespective of the polymer type and  $\bar{M}_w$ . Although PLA oligomers could possibly remain in the continuous liquid, the latter could

Table 5—Characteristics of PLA and PLLA Coacervates

polymer type	polymer concn (% w/w)	DCM (% w/w)	PDMS (% w/w)	coacervate volume (% v/v)	coacervate viscosity <sup>a</sup> (mPa s)	light transmission (Δ% T/h)
L206	1.7	65.1	33.2	9.1	643	5.2
	1.2	48.0	50.8	5.0	5932	19.9
	1.1	41.7	57.2	2.4	nd <sup>b,c</sup>	2.1
	3.3	63.4	33.3	15.7	1724	24.4
	2.5	47.3	50.2	7.1	12011	7.6
	2.1	40.4	57.5	5.8	nd <sup>b,c</sup>	1.1
	6.6	59.4	34.0	23.8	1890	30.5
	5.1	46.0	48.9	13.3	16239	6.1
R206	1.7	66.0	32.3	8.6	1385	32.3
	1.3	48.8	49.9	2.8	9474	3.2
	1.0	37.4	61.6	2.4	nd <sup>c</sup>	7.5

<sup>a</sup> Apparent viscosity at  $D = 500 \text{ s}^{-1}$ . <sup>b</sup> Coacervates tended to gel. <sup>c</sup> nd: not determined because viscosity was too high.

not be analyzed by GPC, as PDMS would interfere with the chromatogram of oligomeric lactides.

**Coacervate Volume and Viscosity**—The addition of PDMS to the PLA or PLGA solutions induced phase separation, which was accompanied by volume and viscosity changes in the coacervate and the continuous liquid. Coacervate volume and viscosity were inversely proportional and depended on polymer concentration and molecular weight (Table 5). The viscosity of PLLA (L 206) and PLA (R 206) coacervates showed a Newtonian behavior for PDMS concentrations up to 35%. In this range (of unstable coacervate droplets), the viscosity was only slightly affected by increasing polymer concentration and attained values of 0.6–1.8 Pa s, depending on the polymer type and molecular weight. Toward the midpoint of the stable coacervate range, the viscosity increased markedly, and the behavior became pseudoplastic. At shear rates  $\leq 500 \text{ min}^{-1}$ , viscosities were 12–17 Pa s, depending on the polymer concentration. At higher polymer concentrations, i.e., 10% initial polymer concentration, the coacervates were too viscous for isolation and handling.

Coacervate droplets of stage 4 of the phase diagram were stabilized by their own viscosity as well as by the increased viscosity of the continuous liquid. Both factors counteracted merging and sedimentation, which was of great importance for controlling microsphere size. Demixing kinetics of the coacervate and continuous liquids was followed by turbidimetric measurements. A pronounced increase in the light transmission was found for coacervation mixtures of relatively low PDMS content. When the PDMS concentration was increased from approximately 33 to 50%, or even to 60%, turbidity first increased markedly and then remained almost constant. An increase in light transmission of 5–10%/h appeared perfectly acceptable for practical purposes, i.e., to prevent merging and sedimentation during the coacervation and hardening processes.

**Effect of Coacervation Conditions on Solvent Residues in Microspheres**—For safety reasons, organic solvent residues in microspheres must be minimized to an acceptable level. Figure 3 shows the impact of coacervation conditions on the solvent residues. Increasing amounts of PDMS in the coacervation mixture diminished the residual hardening agent OMCTS, but led to higher DCM residues. Coacervate droplets produced at low PDMS concentration allowed intimate interaction between the polymer solvent and the hardening agent. As a result, DCM was extracted more efficiently under these conditions, but at the cost of considerable OMCTS inclusion in the microspheres. When raising the amount of PDMS, the viscous polymer network counteracted diffusion and exchange of the components. Hence, residual DCM in microspheres was slightly increased, whereas the OMCTS level dropped considerably.

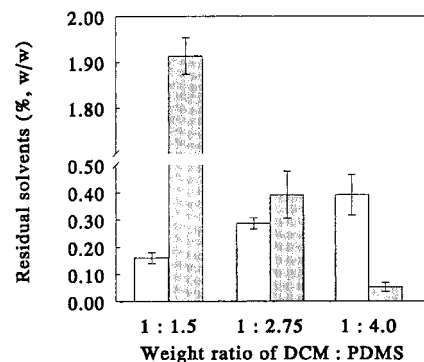


Figure 3—Residual processing liquids in 14.6 kDa D,L-PLA microspheres obtained from different coacervation compositions: polymer solvent DCM (unfilled) and hardening agent OMCTS (filled).

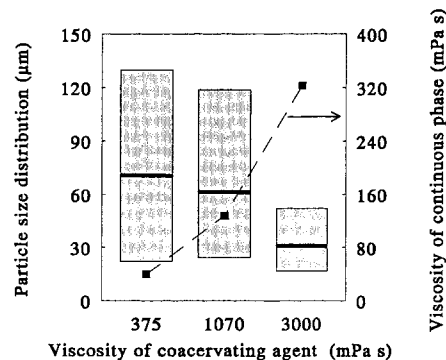


Figure 4—Effect of the coacervating agent (PDMS) viscosity on the viscosity of the continuous phase (dashed line) and the volume weighted particle size distribution of 68.6 kDa PLGA 75:25 microspheres. The bars represent the range of 10–90% undersize diameters and the bold line inside the bar the average particle size.

With respect to the total amount of residuals, i.e., polymer solvent plus hardening compound, a low DCM/PDMS ratio (1:4) produced microspheres with relatively low organic liquid content. To minimize mainly residual DCM, a high solvent:PDMS ratio (1:1.5) appeared more suitable. On the other side, EtAc residues were not analyzed here, but similar findings may be expected, as shown recently in a study on residual solvents in PLA/PLGA microspheres prepared by coacervation.<sup>30</sup> Interestingly, EtAc residuals in microspheres were more than 10-fold higher than DCM residuals, which might be explained, at least partly, by the solubility parameters, but not by the Flory–Huggins model.

**Effect of Coacervation Conditions on Microsphere Particle Size**—Besides hydrodynamic conditions, phase volumes and viscosities were considered important for coacervate droplet size and, hence, the particle size distribution of microspheres. Figure 4 illustrates that the particle size distribution of PLGA 75:25 microspheres became significantly narrower and the sizes smaller when prepared with PDMS of increasing viscosity. This clearly must be a direct consequence of the concomitant viscosity increase of the continuous phase, as indicated in the figure. This change in particle size distribution was mainly due to the considerable reduction of the 90 and 50% undersize values, whereas the 10% undersize limit remained essentially unchanged. Thus, increased shear mediated primarily a breakdown of large coacervate droplets.

Besides the viscosity of the coacervating agent, polymer concentration and polymer  $M_w$  were important parameters influencing the microsphere size distribution. Raising the polymer concentration increased the coacervate volume and viscosity, which in turn produced larger coacervate droplets (Figure 5). On the other side, small-sized microspheres

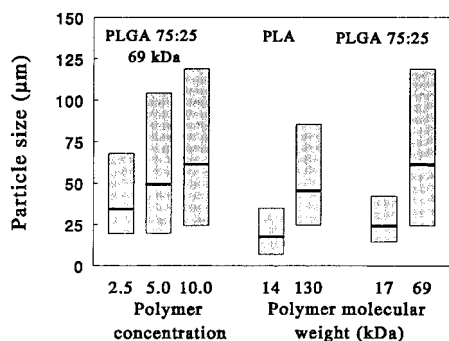


Figure 5—Effect of polymer type, molecular weight, and initial concentration in the solvent on the particle size distribution of microspheres. The 1070 mPa s PDMS was used for phase separation. The bars represent the 10–90% undersize diameters and the bold line inside the bar the average particle size.

were obtained with low  $\bar{M}_w$  polymers. This is ascribed to the low coacervate viscosities obtained with these polymers and to the necessary large volume and high viscosity of the continuous phase.

When considering particle size distributions, interfacial properties of the coacervate and continuous phases have also to be taken into account. Interfacial tension acts as a driving force to minimize the surface free energy of the dispersed phase and, hence, promotes coalescence of coacervate droplets. The coacervated systems generally showed low interfacial tension, as measured by spinning drop tensiometry.<sup>21</sup> This may be explained by the increased adhesion forces generated by solvent partitioning between the coacervate and continuous phases. The interfacial tension of DCM/PLA/PDMS mixtures at two different PDMS concentrations was in the range of 0.9–1.5 mN m<sup>-1</sup>. Slightly lower values (0.6–0.8 mN m<sup>-1</sup>) were obtained in the EtAc/PLA/PDMS dispersions. Thanks to these low interfacial tension values, moderate stirring should be sufficient in the manufacturing process to reduce and control the coacervate droplet size to a desired level and to prevent fast coalescence. Typically, a stirring rate of 350 min<sup>-1</sup> was found adequate to obtain PLGA 75:25 (68.8 kDa) microspheres in the size range of 10–90 µm. Increasing the stirring rate from 350 to 1250 min<sup>-1</sup> did not greatly affect the mean particle size. Therefore, in the systems studied here, stirring rate and interfacial tension were not critical factors for microsphere size.

## Discussion

The results presented in this study show that the organic phase separation process is primarily driven by molecular interaction forces between the compounds present. We consider these molecular interactions as key parameters determining the composition, solvent content, viscosity, interfacial tension, and wetting properties of the coacervate and continuous phases. They are likely to affect the surface characteristics, porosity, particle size, and amount of residual solvent of the final microspheres.

In coacervation, the actual physicochemical properties of a given polymer type greatly influence the phase separation process. Typically, high  $\bar{M}_w$  polymers phase-separate at lower nonsolvent concentration than low  $\bar{M}_w$  polymers. This observation is in agreement with the fundamental prediction that higher  $\bar{M}_w$  polymers are less miscible and, therefore, have a lower concentration limit of phase separation.<sup>22</sup> Similarly, according to Scott's theory, phase-separation of high  $\bar{M}_w$  polymers is expected at lower concentrations of the phase-separating compounds, because the critical polymer 1–polymer 2 interaction parameter is lowered (part 1).<sup>9</sup> Moreover, the homopoly-

mers PLA were less subject to uncontrolled aggregation of coacervate droplets or precipitation than the more hydrophilic PLGA copolymers. Consequently, the range of stable coacervate droplets, also referred to as “stability window”,<sup>6,7</sup> was clearly enlarged with the homopolymers. This is consistent with the findings that increased polymer  $\bar{M}_w$  and hydrophilicity, e.g. due to a larger proportion of low  $\bar{M}_w$  compounds as reflected by larger polydispersity values, lower the polymer solvation by DCM and, consequently, reduce the amount of PDMS needed for phase separation.<sup>6,7</sup> The particular solvation behavior of PLGA 50:50 copolymers has also been revealed by laser light scattering.<sup>23,24</sup> Therefore, it is not surprising that PLA and PLGA 50:50 differ in their phase separation behavior, although their apparent solubility parameters are similar.<sup>25,26</sup> The findings emphasize the importance of detailed polymer characterization to interpret phase separation phenomena.<sup>27</sup>

Phase separation induced by low molecular weight nonsolvents often occurs near the solubility borderline of polymers.<sup>10</sup> Beyond this limit, the increasing difference in solubility parameter between the coacervate phase and the continuous liquid increases the risk of polymer precipitation. This process became critical for PLGA 50:50 and the semicrystalline PLLA, while for the amorphous PLA phase separation occurred well within the solubility range, with a lower risk of precipitation. Polyester coacervation induced by PDMS did not result in polymer fractionation, as the  $\bar{M}_w$  distribution of the coacervates was comparable to that of the polymer powder. This observation strongly supports the mechanism of polymer 1–polymer 2 incompatibility. While the onset of polymer phase separation was primarily determined by the polymer properties, the characteristics of the coacervate were strongly governed by continuous desolvation and partitioning of solvent and PDMS between the two separated phases.

The added amount of PDMS influenced the solvent content and viscosity of the coacervate. At the beginning of the “stability window”, the colloid rich phase exhibited a nearly Newtonian behavior but became pseudoplastic at higher PDMS concentration. Comparable results were reported for an ethylcellulose–chloroform–ethanediol mixture.<sup>28</sup> In the case of hydroxypropylmethylcellulose coacervates, the Newtonian flow was ascribed to minor polymer chain interactions, whereas pseudoplastic behavior was associated with three-dimensional structure.<sup>11</sup> Irrespective of the type of rheological behavior, the concomitant viscosity effect of the continuous and coacervate phases greatly contributes to the stabilization of the coacervate droplets and counteracts agglomeration or uncontrolled precipitation of the colloid.

The physicochemical properties discussed so far also bear consequences on solvent residues in the microspheres. For this type of delivery system, residual solvents are probably a key issue in safety considerations. Typically, highly viscous coacervates are more difficult to desolvate completely by a hardening agent. Correspondingly, such microspheres contain a higher amount of residual polymer solvent and a lower amount of residual hardening agent. This observation is consistent with previous findings showing the importance of a high coacervating agent/solvent ratio for preparing microspheres with low hardening agent residues.<sup>29</sup> Furthermore, the question arises to what extent the coacervating agent is entrapped in microspheres. From a thermodynamic point of view, inclusion of nonsolvents, i.e., coacervating and hardening agents, might be most effectively reduced by minimizing the interaction energy between polymer and nonsolvents ( $\Delta_{int}E$ ; see part 1<sup>9</sup>). However, the actual intermediate interaction between the hardening compounds and the polymer solvents suggests that solvent extraction from the coacervate

by OMCTS or hexane is probably a lengthy and incomplete process. Therefore, nonsolvents with both a low potential for interaction with the polymer and a large molecular volume may be preferable. These properties should counteract the inclusion of the nonsolvents in the free space of the coacervated entangled polymer matrix. Consequently, phase separation driven by polymer 1–polymer 2 incompatibility must be advantageous over processes induced by low molecular weight nonsolvents such as petroleum ether or mineral or vegetable oils. In the former process, the two phases are formed as a consequence of polymer 1–polymer 2 repulsion and each of them is composed of one polymer type. In the latter process, phase separation is induced by polymer desolvation, thereby enhancing the risk of inclusion of nonsolvent within the coacervate droplets. A more detailed study focusing on the aspect of residual solvents in biodegradable microspheres prepared by coacervation has recently been published.<sup>30</sup>

Besides influencing the amount of residual solvents, the viscosity of the coacervation mixture greatly affects the morphology and particle size distribution of microspheres. Predictions of the coacervate droplet size are difficult to make because of the continuous change of phase volumes, viscosity, and interfacial tension. These physicochemical parameters together with the hydrodynamic process conditions all contribute to the particle size distribution.<sup>31–33</sup> Key parameters determining the mean droplet size in a dispersed system were found empirically and compiled in an equation.<sup>34</sup> From this equation, the mean droplet or particle size ( $d$ ) is directly proportional to the ratios of coacervate to continuous phase viscosity ( $\eta_{\text{coac}}/\eta_{\text{cont}}$ ) and volume ( $V_{\text{coac}}/V_{\text{cont}}$ ), to the polymer concentration ( $c$ ), and the interfacial tension ( $\gamma$ ) between both phases, and inversely proportional to the stirring rate ( $N$ ) and the ratio of stirrer to vessel diameter ( $D$ ). The effect of viscosity and interfacial tension on particle size was investigated more closely in other systems.<sup>35,36</sup> The obtained results in those studies agree well with our findings, in as much as the minor effect of interfacial tension and the major effect of the coacervate viscosity on particle size is concerned.

Different concepts have been presented here to describe the silicone oil induced coacervation process of biodegradable polyesters. It has become evident that thermodynamic and other physicochemical considerations may be useful but not sufficient to describe the behavior of the coacervated polymer phase, which in turn will be crucial for the interaction with the drug material to be coated. Finally, we would like to emphasize that this study was not intended to analyze thermodynamically PLA/PLGA phase separation. Clearly, the values given for  $\chi$ ,  $\Delta\delta$ , and  $\Delta_{\text{int}}E$  (Table 3) were not determined by thermodynamic measurements but represent calculated rough estimates with limited validity. Thus, the manufacturing scientist performing coacervation studies for microencapsulation should not rely exclusively on such calculated parameters, but use them as approximate indication for optimizing systems. Clearly, PLA/PLGA phase separation for microsphere preparation is a most complex process which cannot be described and understood sufficiently well by considering only thermodynamic principles.

## References and Notes

1. Benoit, J.-P.; Marchais, H.; Rolland, H.; Vande Velde, V. In *Microencapsulation, Methods and Industrial Applications*; Benita, S., Ed.; Marcel Dekker: New York, 1996; pp 35–72.
2. Fong, J. W. Processes for preparation of microspheres. U.S. Patent, No. 4,166,800, 1979.
3. Sanders, L. M.; Kent, J. S.; McRae, G. I.; Vickery, B. H.; Tice, T. R.; Lewis, D. H. *J. Pharm. Sci.* **1984**, *73*, 1294–1297.
4. Sanders, L. M.; Vitale, K. M.; McRae, G. I.; Mishky, P. B. *J. Controlled Release* **1985**, *2*, 187–195.

5. Lapka, G. G.; Mason, N. S.; Thies, C. Process for preparation of microcapsules. U.S. Patent No. 4,622,244, 1986.
6. Ruiz, J. M.; Tissier, B.; Benoit, J. P. *Int. J. Pharm.* **1989**, *49*, 66–77.
7. Ruiz, J. M.; Busnel, J. P.; Benoit, J. P. *Pharm. Res.* **1990**, *7*, 928–934.
8. Nihant, N.; Grandfils, C.; Jérôme, R.; Teyssié, Ph. *J. Controlled Release* **1995**, *35*, 117–125.
9. Thomasin, C.; Merkle, H. P.; Gander, B. *J. Pharm. Sci.* **1998**, *87*, 259 (preceding paper in this issue).
10. Robinson, D. H. *Drug Dev. Ind. Pharm.* **1989**, *15*, 2597–2620.
11. Weiss, G. Mikroverkapselung von Ibuprofen mit magensaftresistanten Polymeren durch einfache Koacervation; Ph.D. Thesis, University of Regensburg, D.-Regensburg, 1991.
12. Moldenhauer, M. G.; Nairn, J. G. *J. Controlled Release* **1992**, *17*, 205–218.
13. Gander, B.; Merkle, H. P.; Nguyen, V. P.; Hô Nam-Trân J. *Phys. Chem.* **1995**, *99*, 16144–16148.
14. Thomasin, C.; Corradin, G.; Men, Y.; Merkle, H. P.; Gander, B. *J. Controlled Release* **1996**, *41*, 131–145.
15. Technical information from Dow Corning, Midland, MI.
16. Van Krevelen, D. W. *Properties of polymers*, 3rd ed.; Elsevier: Amsterdam, 1990; pp 189–225; 287–320.
17. Burrell, H. In *Polymer Handbook*; Brandrup, J., Immergut, E. H., Eds.; Wiley: New York, 1966; p 341.
18. Klimisch, H. M. In *The Analytical Chemistry of Silicones*; Lee Smith, A., Ed.; Wiley: New York, 1991; pp 117–121.
19. Baney, R. In *Structure–Solubility Relationships in Polymers*; Harris, F. W., Seymour, R. B., Eds.; Academic Press: New York, 1977; pp 225–231.
20. Lide, D. R. *CRC Handbook of Chemistry and Physics*, 75th ed.; CRC Press: Boca Raton, FL, 1994; p 6–151.
21. Thomasin, C.; Merkle, H. P.; Gander, B. *Int. J. Pharm.* **1997**, *147*, 173–186.
22. Dobry, A.; Boyer-Kawenoki, F. *J. Polymer Sci.* **1947**, *2*, 90–100.
23. Bendix, D. *Proc. Int. Symp. Controlled Release Bioact. Mater.* **1990**, *17*, 248–249.
24. Rafler, G.; Jobmann, M. *Pharm. Ind.* **1994**, *56*, 565–570.
25. Siemann, U. *Proc. Int. Symp. Controlled Release Bioact. Mater.* **1985**, *12*, 53–54.
26. Siemann, U. *Eur. Polym. J.* **1992**, *28*, 293–297.
27. Donbrow, M. In *Microcapsules and Nanoparticles in Medicine and Pharmacy*; Donbrow, M., Ed.; CRC Press: Boca Raton, FL, 1992; pp 20–23.
28. Nixon, J. R.; Nimmanit, U. *J. Microencapsulation* **1985**, *2*, 103–110.
29. Lewis, D. H.; Sherman, J. D. Low residual solvent microspheres and microencapsulation process. PCT patent application, No. WO 89/03678, 1989.
30. Thomasin, C.; Johansen, P.; Alder, R.; Bemsel, R.; Hottinger, G.; Altorfer, H.; Wright, A. D.; Wehrli, E.; Merkle, H. P.; Gander, B. *Eur. J. Pharm. Biopharm.* **1996**, *42*, 16–24.
31. Kipke, K. D. *Verfahrenstechnik* **1981**, *15*, 563–566.
32. Sweeney, E. T. *An Introduction and Literature Guide to Mixing; BHRA Fluid Engineering Series*, Bedford, 1978; Vol. 5, pp 5–40.
33. Oldshue, J. Y. In *Fluid Mixing Technology, Chemical Engineering*; Oldshue, J. Y., Ed.; McGraw-Hill Publications: New York, 1983; pp 125–140.
34. Arshady, R. *Polym. Eng. Sci.* **1989**, *29*, 1746–1757.
35. Arai, K.; Konno, M.; Matunaga, Y.; Saito, S. *J. Chem. Eng. Jpn.* **1977**, *10*, 325–329.
36. Sanghvi, S. P.; Nairn, J. G. *J. Microencapsulation* **1992**, *9*, 215–227.
37. Barton, A. F. M. *Handbook of Solubility Parameters and Other Cohesion Parameters*, 2nd ed.; CRC Press: Boca Raton, FL, 1991; pp 95–111.
38. Barton, A. F. M. *Handbook of Polymer–Liquid Interaction Parameters and Solubility Parameters*; CRC Press: Boca Raton, FL, 1990; pp 125–147; 293–296.
39. Drago, R. S.; Dadmun, A. P.; Vogel, G. C. *Inorg. Chem.* **1993**, *32*, 2473–2479.
40. Flory, P. J. *Principles of Polymer Chemistry*, Cornell University Press: Ithaca, NY, 1953; pp 541–594.

## Acknowledgments

The authors thank Dr. Ernst Wehrli, Laboratory for Electron Microscopy I, ETH (Zurich, Switzerland), for making the SEM-micrographs and Dr. Hô Nam-Trân, School of Pharmacy, University of Lausanne (Lausanne, Switzerland), for helpful discussion on thermodynamic aspects.

JS970048J